

Published in final edited form as:

Oncogene. 2021 February 01; 40(6): 1091–1105. doi:10.1038/s41388-020-01584-6.

STAT3 promotes melanoma metastasis by CEBP-induced repression of the MITF pathway

Alexander Swoboda^{1,2,*}, Robert Soukup^{3,*}, Oliver Eckel^{2,3}, Katharina Kinslechner³, Bettina Wingelhofer^{1,2}, David Schörghofer³, Christina Sternberg⁴, Ha T. T. Pham^{1,2}, Maria Vallianou³, Jaqueline Horvath^{1,5}, Dagmar Stoiber^{1,5}, Lukas Kenner^{1,6,7,8}, Lionel Larue⁹, Valeria Poli¹⁰, Friedrich Beermann¹¹, Takashi Yokota¹², Stefan Kubicek¹³, Thomas Krausgruber¹³, André F. Rendeiro¹³, Christoph Bock^{13,14,15}, Rainer Zenz¹⁶, Boris Kovacic³, Fritz Aberger⁴, Markus Hengstschläger³, Peter Petzelbauer¹⁷, Mario Mikula^{3,#}, Richard Moriggl^{1,2,#}

¹Ludwig Boltzmann Institute for Cancer Research, Vienna, Austria ²Institute of Animal Breeding and Genetics, University of Veterinary Medicine, Vienna, Austria ³Center for Pathobiochemistry and Genetics, Institute of Medical Genetics, Medical University of Vienna, Vienna, Austria ⁴Department of Biosciences, Cancer Cluster Salzburg, University of Salzburg, Austria ⁵Institute of Pharmacology, Center of Physiology and Pharmacology, Medical University of Vienna, Vienna, Austria ⁶Institute of Clinical Pathology, Medical University of Vienna, Vienna, Austria ⁷Unit of Pathology of Laboratory Animals, University of Veterinary Medicine, Vienna, Austria ⁸CBMed Core Lab2, Medical University of Vienna, Vienna, Austria ⁹Institute Curie, Normal and Pathological Development of Melanocytes, CNRS UMR3347, INSERM U1021 Equipe labellisée, Orsay, France ¹⁰Department of Molecular Biotechnology and Health Sciences, University of Torino, Torino, Italy ¹¹ISREC, Swiss Federal Institute of Technology in Lausanne, Lausanne, Switzerland ¹²Department of Stem Cell Biology, Graduate School of Medical Sciences, Kanazawa University, Kanazawa, Ishikawa, Japan ¹³CeMM Research Center for Molecular Medicine of the Austrian Academy of Sciences, Vienna, Austria ¹⁴Department of Laboratory Medicine, Medical University of Vienna, Vienna, Austria ¹⁵Max Planck Institute for Informatics, Saarland Informatics Campus, Saarbrücken, Germany ¹⁶Institute of Cancer Research, Medical University of Vienna, Vienna, Austria ¹⁷Department of Dermatology, Skin and Endothelium Research Division (SERD), Medical University of Vienna, Vienna, Austria

Abstract

Metastatic melanoma is hallmarked by its ability of phenotype switching to more slowly proliferating, but highly invasive cells. Here, we tested the impact of signal transducer and

Users may view, print, copy, and download text and data-mine the content in such documents, for the purposes of academic research, subject always to the full Conditions of use:http://www.nature.com/authors/editorial_policies/license.html#terms

#Equal corresponding Authors: Dr. Richard Moriggl, Institute of Animal Breeding and Genetics, University of Veterinary Medicine, Vienna, Veterinärplatz 1, A-1210 Vienna, Austria, richard.moriggl@vetmeduni.ac.at, Phone: +43 1 250775622, Fax: +431250775693; Dr. Mario Mikula, Institute of Medical Genetics, Medical University Vienna, Vienna, Waehringstrasse 10, A-1090, Vienna, mario.mikula@meduniwien.ac.at, Phone: +43 1 4016056540, Fax: +43140160956501.

*These authors contributed equally to this work.

Conflict of interest The authors declare that they have no conflict of interest.

activator of transcription 3 (STAT3) on melanoma progression in association with melanocyte inducing transcription factor (MITF) expression levels. We established a mouse melanoma model for deleting *Stat3* in melanocytes with specific expression of human hyperactive *NRAS^{Q61K}* in an *Ink4a* deficient background, two frequent driver mutations in human melanoma. Mice devoid of *Stat3* showed early disease onset with higher proliferation in primary tumors, but displayed significantly diminished lung, brain and liver metastases. Whole genome expression profiling of tumor-derived cells also showed a reduced invasion phenotype, which was further corroborated by 3D melanoma model analysis. Notably, loss or knockdown of *STAT3* in mouse or human cells resulted in up-regulation of MITF and induction of cell proliferation. Mechanistically we show that STAT3-induced *CEBPa/b* expression was sufficient to suppress *MITF* transcription. Epigenetic analysis by ATAC-seq confirmed that *CEBPa/b* binding to the *MITF* enhancer region silenced the *MITF* locus. Finally, by classification of patient-derived melanoma samples, we show that STAT3 and MITF act antagonistically and hence contribute differentially to melanoma progression. We conclude that STAT3 is a driver of the metastatic process in melanoma and able to antagonize *MITF* via direct induction of CEBP family member transcription.

Introduction

Melanoma is a very aggressive form of skin cancer, with >76.000 new cases diagnosed annually in the US [1]. Stage I and stage II lesions can be successfully removed by surgery, but metastasized melanomas are challenging to treat, leading to an estimated 10.000 deaths in the US annually [1]. The current prognosis of advanced melanoma remains poor despite the success of immune- and targeted therapy. The plasticity of melanoma, which describes the ability of melanoma cells to switch multiple times from a proliferative to an invasive state and *vice versa* without the need for additional mutations, is in part responsible for the low curation rates [2, 3]. This process is also called phenotype-switching and involves the Microphthalmia-associated Transcription Factor (MITF) [4]. MITF is essential for melanocyte development, homeostasis and pigmentation response [5, 6]. MITF controls differentiation, survival and proliferation and its expression is also transcriptionally regulated by SOX10, a transcriptional activator important for neural crest development [7]. High MITF expression marks melanoma cells with a proliferative, but non-invasive phenotype. In contrast, melanoma cells expressing low MITF protein represent increased invasive and metastatic capacity [2, 8–10]. These findings exemplify an essential role for MITF in melanoma biology.

Although the transcriptional regulation of MITF is well described, the interplay with STAT3 in cancer biology has so far not been established. STAT3 shows enhanced tyrosine phosphorylation in melanoma, catalyzed via JAK, SRC or growth factor tyrosine kinase family members [11]. Reports on inhibition of STAT3 by siRNA or expression of a dominant negative form of STAT3 in melanoma xenografts postulated an oncogenic role of STAT3 in melanoma progression [12, 13]. However, treatment with STAT3 activators like Oncostatin M (OSM) or IL-6 resulted in tyrosine phosphorylation of STAT3 (pYSTAT3) and decreased proliferation in melanoma cell line studies, suggesting a tumor suppressor role for STAT3 in melanoma progression [14, 15]. Complete genetic deletion studies for STAT3 in melanoma are still missing, whereas in prostate, lung and colorectal carcinomas, tumor

suppressive roles were associated with STAT3 function depending on the mutational context [16–18]. Importantly, it is not clear whether STAT3 plays a role in phenotype-switching towards invasive melanoma.

Here, we utilized a genetic model of spontaneous melanoma formation based on relevant driver mutations for human melanoma initiation and progression. Mice carrying melanocyte-specific expression of the *NRAS*^{Q61K} oncogene in an *Ink4a*-deficient background were generated [19, 20]. Additionally, our mouse model allows for conditional melanocyte-specific deletion of *Stat3* [21]. We show that mice lacking *Stat3* expression in melanomas have an accelerated visible tumor onset *in vivo* and exert a higher proliferating cell nuclear antigen (PCNA) labeling. In contrast, metastasis formation from *Stat3* knockout primary tumors was severely impaired when analyzing lung, brain and liver tissue. Next, STAT3 function was evaluated mechanistically using tumor derived cell lines, where we performed whole genome expression analysis combined with ATAC-seq profiling. We found, that STAT3 antagonizes MITF expression through elevated expression of CAAT Box Enhancer Binding Protein (CEBP) family members. Remarkably, *in silico* data mining of melanoma patient samples also revealed a negative correlation of *CEBPa/b* with *MITF* mRNA expression values. *STAT3* knockdowns in human melanoma confirmed the antagonistic action on MITF expression with consequences for changed proliferation and invasion. We conclude that loss or down-regulation of STAT3 inhibits melanoma metastasis and that in response MITF is up-regulated. We propose that the complex interplay of these two master-regulators, which both act as oncogenes in melanoma progression, determines clinical outcome and patient fate.

Materials and Methods

Animals

Mice carrying the *Stat3*^{flxed} allele [21] were crossed with transgenic mice carrying melanocyte-specific expression of the *NRAS*^{Q61K} oncogene in an INK4A-deficient background [19, 22] and tyrosinase *Cre* [23]. Human *NRAS*^{Q61K} and *Cre* are targeted to the melanocyte lineage by tyrosinase regulatory sequences. Compound *Tyr::NRAS*^{Q61K} *Ink4a*^{-/-}; *Stat3*^{flx/flx}; *Tyr::Cre* mice were termed Stat3^{fl} for simplified reading and maintained on a C57BL/6Jx129/Sv background. In all experiments described, sex ratio was equal and littermates lacking *Tyr::Cre* were used as controls and termed Stat3^{fl}. For *in vivo* experiments the number of biological replicates is indicated in each figure shown. Animals were randomly assigned to groups, no blinding was applied. All mice were bred and maintained under standardized conditions at the Decentralized Biomedical Facility of the Medical University Vienna according to an ethical animal license protocol complying with the Austrian law and approved by the “Bundesministerium für Wissenschaft und Forschung” (BMWF-66009/0281-I/3b/2012).

Cell lines

Mouse melanoma cell lines were established from lymph nodes of diseased mice (25–30 weeks of age) by single cell dissociation and culturing. Multiple individual primary pools of cell lines per Stat3^{fl} and Stat3^{fl} melanoma cell genotype were generated, upon which we

selected two pools each for further detailed analysis. Gene lists for STAT3 targets are shown in Supplementary Table 1 and the MITF pathway members are shown in Supplementary Table 2. The primers used in this study are listed in Supplementary Table 3. Human *BRAF* mutated cell lines WM793B, 451Lu and WM35 were freshly bought from ATCC. All cell lines were cultivated under standard conditions (95% humidity, 5% CO₂, 37°C) and maintained in DMEM supplied with 10% Fetal Bovine Serum, 10 U/ml Penicillin, 10 µg/ml Streptomycin, 2 mM L-Glutamine (all from Gibco, Thermo Fisher, Waltham, MA) and 2 µg/ml Ciprofloxacin (Sigma-Aldrich, St. Louis, MO). Cells were routinely tested for mycoplasma contamination.

Immunohistochemistry and immunofluorescence

For immunohistochemistry 4µm tissue sections were deparaffinized and rehydrated in graded ethanol dilutions, after which antigen retrieval was carried out. Staining was performed using the ABC kit according to the manufacturer's instructions (Novocastra, Wetzlar, Germany). As substrate 3-amino-9-ethylcarbazole was used (Agilent Technologies) and imaging was done with an Olympus BX63 microscope. The intensity of staining was evaluated by two blinded, board certified pathologists. For immunofluorescence cells were grown on chamber slides and fixed in 4% formaldehyde. After staining with primary and corresponding secondary antibodies imaging was done on a Leica TCS SP8 Microscope. Signal intensity was calculated by measuring pixel density in image J for CEBP positive nuclei and control nuclei. The antibodies used in this study are listed in Supplementary Table 4 and 5. Full size western blots are shown in Supplementary Figure 1a-d.

Clinical Samples

All melanoma samples were obtained from the Department of Dermatology, General Hospital Vienna. In each case, pathological diagnosis was made after elective surgery for malignant melanoma. Human tissue samples were collected after signed, informed consent was provided and approval for studies was obtained from Ethics Committee of the Medical University of Vienna, EK 405/2006, extension 11/10/2016. Additional materials and methods are provided in Supplementary Information.

Results

Tissue specific loss of STAT3 enabled earlier tumor onset

To study the effect of STAT3 loss in melanoma we used transgenic mice that allow for conditional deletion of *Stat3* by *Cre-loxP* technology. To closely mimic human cutaneous melanoma progression, we employed a genetic mouse model driven by melanocyte specific hyperactive human *NRAS^{Q61K}* that has been further crossed to an *INK4a*-deficient background. Melanoma that carry *NRAS^{Q61K}*, lost p16^{INK4A} and p19^{ARF} and deleted *Stat3* (Tyr::NRAS^{Q61K}Ink4a^{-/-}Stat3^{fllox/fllox}Tyr::Cre) are further termed Stat3^{-/-}, control melanoma expressing STAT3 are termed Stat3^{fl} (Fig. 1a). Melanocyte specific CRE expression was described to recombine *loxP* sites from E10.5 onwards in development [24]. Consistently, mice developed tumors on their skin starting from 12 weeks of age (Fig. 1b). Disease onset, defined as appearance of palpable tumors with a size bigger than 1 mm, was significantly accelerated in the Stat3^{-/-} group (Fig. 1c).

As expected STAT3 was lost in mouse skin melanomas when tested by immunohistochemistry (Fig. 1d). PCNA staining revealed that primary Stat3^{fl} tumors displayed increased proliferative activity compared to Stat3^{fl} tumors (Fig. 1e). Loss of *Stat3* could affect expression from the *Stat5a* and *Stat5b* gene locus, which resides in proximity on the same chromosome. Hence, we further investigated their expression and nuclear localization by antibody staining, but no significant difference was observed (Supplementary Fig. S2a, b).

Expression profiling revealed pigmentation and MITF pathway induction upon loss of STAT3

We isolated tumor cells from melanoma positive lymph nodes of the Stat3^{fl} and Stat3^{fl} mice and selected for melanoma cells by continuous culturing. Cells were uniformly positive for the melanoma marker S100b (Supplementary Fig. S2c). Control cells showed basic STAT3 activity according to Y705 phosphorylation, while with IL-6 stimulation enhanced STAT3 activity was observed (Fig. 2a). Importantly, Stat3^{fl} cells showed complete loss of STAT3 expression and STAT3 Y705 phosphorylation in all conditions as detected by Western blotting.

Next, we performed Affymetrix whole transcriptome microarray mRNA analysis followed by gene set enrichment analysis (GSEA) under basal growth conditions or during stimulation with murine IL-6 or OSM. Loss of *Stat3* resulted in significant reduction of STAT3 target gene expression and importantly, Stat3^{fl} cells displayed augmented MITF pathway activation (Fig. 2b). As expected cytokine stimulation had no effect on STAT3 target or MITF pathway gene expression in knockdown cells (Fig. 2c, d and Supplementary Fig. S3a-c). Increased MITF activity was validated by measuring absorbance of melanin in conditioned medium of STAT3 wild type and knockout cells (Fig. 2e). Additionally we detected increased melanin amounts in primary tumors lacking *Stat3* (Fig. 2f). We conclude that loss of *Stat3* is accompanied by up-regulation of the MITF pathway resulting in increased pigmentation of cells and tissue.

Invasion and metastatic outcome are reduced upon loss of *Stat3*

Gene set enrichment analysis, including proliferative and invasive melanoma signatures, were performed to identify STAT3 related phenotypes (Fig. 3a). We found that Stat3^{fl} cells resembled MITF-driven proliferative gene signatures, which were identified in two large and independent melanoma cohort studies [2, 10, 25, 26]. In contrast, Stat3^{fl} cells were closely related to the described invasive signatures [10, 25] and the hallmark EMT dataset defined by the GSEA team [27].

To validate our whole genome expression profiling we performed *in vitro* assays, where we found enhanced 3D-proliferation, but abrogated invasion and migration in Stat3^{fl} cells (Fig. 3b, c). Our data implies that STAT3 fulfills an important function in RAS-transformed melanoma promoting invasion and migration. Tumor allografts of Stat3^{fl} cells were more compact, with higher cellular density and allografts showed little to no significant invasion of epidermal tissue. In contrast, Stat3^{fl}-derived tumors were de-differentiated with fibroblastoid morphology, displaying high invasion into murine epidermis (Fig. 3d).

Next, lungs of 40 week-old mice were stained for S100b to visualize metastasis formation. Importantly, *Stat3* deletion significantly reduced the overall number of metastatic lung colonies (Fig. 3e, f). Furthermore, we screened brains and livers from sacrificed animals for macroscopic tumor colonization. Brain metastasis was reduced by 23% and liver metastasis was reduced by 15% in the *Stat3* knockout animals (Fig. 3g). Additionally, we performed KI67 staining and identified a significant increase in labeling of metastatic lesions of knockout animals (Fig. 3h). In summary, knockout animals showed earlier onset of disease, increased PCNA expression in primary tumors and increased KI67 amounts in metastatic samples, but knockout cells also displayed decreased invasive capacities and less metastasis forming activity in distal organs. Next we asked how these different properties impact the overall survival of mice. Therefore we estimated the survival curve from cage side observations and the derived Kaplan Meier plot showed that survival between both groups of animals was comparable (Supplementary Fig. S4). This indicated that although wild type and knockout mice exhibited different phenotypes, in the end tumor burden, regarded as the sum of tumor spread and tumor growth, resulted in a similar outcome in life expectancy.

We continued to further analyze whole genome expression profiling, which revealed a set of five important de-regulated receptor tyrosine kinases: Three of them, *Platelet-Derived Growth Factor Receptor alpha and beta (PDGFRa/b)* and *Epidermal Growth Factor Receptor (EGFR)* displayed decreased mRNA expression in the *Stat3* group (Fig. 4a and Supplementary Fig. S5). Two receptor tyrosine kinases, *MET* and *cKIT*, were increased (Fig. 4b). Accordingly, PDGFRb and EGFR were highly expressed in immunostainings of primary *Stat3^{fl}* mouse melanomas, whereas *Stat3* tumors showed increased expression of *MET* (Fig. 4c). PDGFRb and EGFR were also highly expressed in wild type primary tumors, whereas *MET* was predominantly expressed in corresponding *Stat3* knockout samples (Supplementary Fig. S6). To dissect the regulatory basis for the observed changes in the cell transcriptomes, we performed chromatin profiling using ATAC-seq with a focus on the *cKit* and *Pdgfrb* locus in *Stat3^{fl}* and *Stat3* melanoma cells. Chromatin accessibility at the *cKit* promoter region was increased only in *Stat3* and conversely the *Pdgfrb* promoter was only accessible in *Stat3^{fl}* cells (Fig. 4d, e). This indicates, that the loss of STAT3 leads to epigenetic changes accompanied by the observed strong changes in gene expression patterns.

Assessment of chromatin accessibility reveals reciprocal expression between CEBPs and MITF

To investigate the mechanisms underlying the regulation of MITF by STAT3, we reasoned that STAT3 or its downstream targets could repress MITF. To test this hypothesis, we investigated regulatory elements of the proximal *Mitf* promoter region by ATAC-seq. We found that *Stat3^{fl}* cells displayed chromatin accessibility in a regulatory element in close proximity of the *Mitf* gene, which contained a *CEBPa/b* binding element (Fig. 5a, b). Access at this site was specifically lost in *Stat3* cells. Contrary, *Stat3* cells displayed an increased accessibility at a regulatory element containing a *SOX10* binding element that was absent in *Stat3^{fl}* cells.

The CEBP transcription factors are well-known downstream targets of STAT3 and we could identify strong inhibition of *Cebpa/b/d* mRNA expression after *Stat3* knockout. Moreover, via protein analysis we found significantly increased CEBPa/b in a STAT3-dependent way and we could confirm reciprocal expression with MITF and SOX10 (Fig. 5c). Next, we introduced a 4-OH-tamoxifen inducible STAT3ER^{T2} construct [28] into *Stat3* murine melanoma cells. Addition of 4-OH-tamoxifen led to an increased expression of *Cebpa/b* mRNA as measured by RT-PCR analysis (Fig. 5d). Expression and activation of the STAT3ER^{T2} fusion protein by 4-OH-tamoxifen was confirmed by Western blot analysis (Supplementary Fig. S7a). Induced STAT3 activity led to a reciprocal down-regulation of MITF pathway associated genes and *Mitf*, *Met*, *cKit*, *Tyr* were significantly repressed. Importantly, exogenous *Cebpa* expression in *Stat3* melanoma cells and subsequent mRNA quantification led to a significant reduction in *Mitf* and *Met* expression, altering levels of these genes to approximately 50% of control cells (Fig. 5e). To validate these findings CEBPa or CEBPb were ectopically over-expressed and MITF expression was monitored on single cell level using microscopy. Melanoma cells devoid of STAT3 showed increased MITF protein expression, but when transfected with CEBPa or CEBPb then MITF levels were significantly reduced (Fig. 5f and Supplementary Fig. S7b and S8a, b). We conclude that STAT3-driven CEBP family member expression is responsible for repression of MITF mRNA and protein levels.

To test, whether our findings also apply for human melanoma cell lines, we performed stable lentiviral shRNA mediated knockdown of *Stat3* in 451Lu, WM793B and WM35 cells. All three cell lines have the *INK4A* locus deleted and are driven by a BRAF^{V600E} mutation. Evaluation of the knockdown was performed via RT-PCR (Fig. 6a). Consistent with our murine data, we observed up-regulation of *MITF*, *MET*, *SOX10* and *TYR* on mRNA level (Fig. 6b). Furthermore, cells devoid of *Stat3* showed increased cell proliferation (Fig. 6c). MITF and SOX10 were also up-regulation on protein level (Fig. 6d). Additionally increased clonogenic growth capabilities were observed (Fig. 6e). To discriminate whether the increase in cell number is due to increased cycling of cells or due to decreased apoptosis we quantified KI67 and cleaved caspase 3 amounts in the respective cell lines (Fig. 6f). To further validate and to address the clinical relevance of our findings, we evaluated publicly available expression data sets from the Gene Expression Omnibus (GEO) and The Cancer Genome Atlas (TCGA) databases. This analysis revealed a strong negative correlation between *MITF* and *CEBPA* as well as between *MITF* and *CEBPB* expression (Fig. 6g).

Validation of STAT3 expression signatures in human clinical samples

To assess the clinical relevance of the relationship between MITF and CEBPa/b, we analyzed publicly available datasets (GEO accession GSE19234 and TCGA data from Cutaneous Melanoma). Using the online tool SurvExpress [29] samples were sorted according to the expression level of *STAT3*, *CEBPA*, *CEBPB* and *MITF* to generate equal sized low- and high-risk groups, to achieve the maximum possible difference in estimate patient survival times (Fig. 7a). The high-risk group was defined by high levels of *MITF* in combination with low *STAT3*, *CEBPA* and *CEBPB* levels. As expected, Kaplan Meier survival analysis showed significant differences in survival probability between high- and low-risk groups in both cohorts (Fig. 7b). We also analyzed survival of patients based solely

on STAT3 expression in the TCGA dataset and patient cumulative survival is predicted with $p=0.017$ (Supplementary Fig. S9a, b). To validate our findings in human patient samples we analyzed a cohort of 25 primary melanoma tumors and 96-130 melanoma metastases for STAT3 and MITF antibody mediated staining intensities. Primary tumors compared to metastases showed higher levels of STAT3 protein, while MITF levels were higher in metastases than in primary tumors (Supplementary Fig. S10a, b and S11). To indicate active STAT3 we focused on nuclear STAT3 localization and we used consecutive sections to analyze co-occurring amounts of MITF and KI67 (Fig. 7c). Representative stained samples are shown (Fig. 7d).

In summary, we conclude that expression of CEBP family members depends on expression of STAT3 protein. Upon *Stat3* deletion, *Cebpa*, *Cebpb* and *Cebpd* levels decrease, translating also in diminished protein expression and resulting in increased expression of MITF. This process leads to abrogated invasion and to diminished metastasis formation as illustrated in the summary schematic (Fig. 7e).

Discussion

We identified STAT3 as a critical regulator in the dynamic process of melanoma progression. Using a NRAS-driven mouse cutaneous melanoma model, devoid of INK4A tumor suppressors, we found that on the one hand STAT3 facilitated tumor cell spreading, while on the other hand STAT3 repressed MITF levels and it also diminished slightly proliferation of tumor cells. This indicates that STAT3 represents an important novel regulator in the complex relationship between phases of invasion and alternating phases of proliferation. Our findings have implications for the diagnosis as well as for therapeutic treatment of melanoma.

Tumor cells undergo progression and metastatic spread by adopting different biologic programs like proliferation, invasion, extravasation and distant colonization known as the invasion-metastasis cascade [30]. During this process, the alteration of proliferative phases with low proliferative phases is of paramount importance [2]. Here we propose that STAT3 is a key molecule able to regulate this transition. Analysis of STAT3 mutations in human solid cancers, including melanoma, revealed a low mutation frequency (28). Loss of function mutations like nonsense and frameshift mutations were even less frequent compared to missense mutations [31]. These data support the notion that STAT3 is not a major target for somatic mutations in solid tumors, but subjected to extensive upstream regulation. Hence, levels of STAT3 activity can change according to the cellular context and furthermore influence melanoma progression. Likewise tumor cells with active STAT3 are prone for increased invasion and metastasis, for example at the invasive tumor border, while cells with down-regulated or no STAT3 show enhanced proliferation, for example at the metastatic site. Here, we provide evidence that genetic deletion of the *STAT3* locus reduces the plasticity of melanoma cells and inhibits the transition from a proliferative phenotype to an invasive phenotype.

We have shown that loss of STAT3 expression is accompanied with increased proliferation as loss of STAT3 caused an earlier disease onset in mice consistent with a pronounced

proliferative signature marked by augmented MITF expression. In human cells knockdown of STAT3 also resulted in up-regulation of MITF and induction of cell proliferation and this could be explained by STAT3 interfering with malignant melanoma growth through antagonizing MITF. When we further compare histology data from our mouse model with findings from our human study we can observe that the increased cell proliferation in STAT3 knockout mouse tumors is reflected in elevated KI67 staining of human melanoma samples, which also show decreased STAT3 expression. Interestingly increased labeling for KI67 as well as mitotic counts are robust prognostic predictors for worsening of survival in melanoma-bearing individuals [32, 33]. Both, our mouse as well as human studies show that tumors low in STAT3 display high amounts of MITF and importantly, metastatic melanoma patients with MITF amplifications show a dramatic decrease in survival probabilities compared to normal MITF status [34]. Hence, our bioinformatics analysis exemplifies that low amounts of STAT3 are associated with the so called high risk group, probably due to high proliferation, whereas melanoma cells high in STAT3 are low in proliferation and form the so called low risk group. MITF is a master transcription factor during melanocytic differentiation and controls lineage specific proliferation [35]. We suggest that the MITF repression is mediated by increased CEBPA and CEBPB amounts. CEBP family members are well-established downstream targets of STAT3 [36]. Binding of SOX10 to the MITF promoter positively regulates expression [37, 38], while binding of CEBPA inhibits MITF expression in myeloid cells [39]. Here we show that rescuing of Stat3 melanoma cells by reactivation of the STAT3 pathway or by forced expression of *CEBPa/b* also repressed *Mitf* mRNA production. Furthermore, we show that loss of STAT3 diminished expression of CEBP family members and CEBP binding motifs were less accessible as determined by ATAC-seq at the *Mitf* locus. Analysis of human expression datasets showed that high *MITF* correlated with low *STAT3* and *CEBPa/b* levels. We have shown that STAT3 was essential for the establishment of an EMT signature according to whole genome expression profiling. Tumor invasion and migration activity was abrogated upon STAT3 loss, reminiscent of a loss of an EMT-like phenotype. Additionally, we found EGFR and PDGFR up-regulation in wild type compared to STAT3 knockout melanomas. PDGFR-beta is, for example, strongly expressed in pericytes and its expression in epithelial cells is regarded as a marker for the EMT phenotype [40]. Our conclusion regarding STAT3 as a metastasis driver is strengthened by recent reports, which describe STAT3 activity in melanoma cells as a driver for up-regulation of invasion-related genes and as a major factor in the transition towards a mesenchymal phenotype during EMT-like processes [41]. Additionally, DNp73 was shown to initiate metastasis in melanoma by activating STAT3 signaling [42]. Likewise, STAT3 was also shown to drive pancreas cancer metastasis to the liver [43] and STAT3 inhibition served as an effective strategy to reduce invasion and migration of cells [12, 44].

The presence of an EMT phenotype has not only been associated with invasion and migration, but also with an increased stemness of tumor cells [45]. Interestingly, STAT3 controls stability of NANOG and SOX2, which are important stem cells transcription factors [46, 47]. STAT3 is also required for the viability of cancer stem cells in different tumor types including melanoma [48–51].

Treatment of melanoma currently focuses on the use of BRAF and MEK inhibitors, as well as on the remarkable success with blockade of immune checkpoint inhibitors. Unfortunately

patients still show low response rates towards anti-melanoma therapy, which has been attributed to the pronounced EMT-like phenotype [52, 53]. Specifically EMT in tumor patients is considered as a major factor in the development of resistance towards tyrosine kinase blockers [4] and for escaping PD-1 immunotherapy treatment [54]. Mechanistically resistance to vemurafenib treatment can occur when patients are low in MITF which leads, in line with our data, to corresponding up-regulation of EGFR [55]. Therefore, involvement of STAT3 in the EMT process, in enhancing stemness, as well as in immune evasion-phenotype of tumor cells, could have significant implications for future melanoma therapy.

Our human STAT3 melanoma data pinpoint to a possible novel therapeutic opportunity. Hence, we suggest that targeting of STAT3 would prevent repetitive switching of tumor cells into an invasive, low proliferative and more treatment resistant cell population. To counteract the rise in proliferation after STAT3 inhibition a combinatory treatment approach to also suppress MITF can be envisioned. This could be achieved by interfering with tumor differentiation or by decreasing the levels of SR-BI in melanoma [56, 57]. Already in clinical use are HDAC inhibitors, which also show suppression of MITF [58]. Therefore, Panobinostat and Vorinostat are candidate drugs, currently being tested as adjuvant therapy (NCT02032810), or as stand-alone treatment (NCT02836548) after BRAF^{V600E} inhibitor resistance (data from *clinicaltrials.gov*). Additionally, clinically approved tyrosine kinase inhibitors such as Dasatinib and Nilotinib, inhibiting cKIT/PDGFR, or Crizotinib and Cabozantinib, inhibiting cMET/ALK, could be used in combination with STAT3 inhibition.

Our findings imply that STAT3 represents a vulnerable node enabling melanoma transition from proliferation to migration and invasion. We conclude that a balanced expression of STAT3 and MITF controls melanoma fate and we propose that the main role of STAT3 is to promote invasion and metastatic spread.

Supplementary Material

Refer to Web version on PubMed Central for supplementary material.

Acknowledgments

We thank Safia Zahma, Birgit Schütz, Eva Bauer, Michaela Schleder and Karin Neumüller for excellent technical assistance. We also thank the Biomedical Sequencing Facility at CeMM for assistance with next generation sequencing. VP was supported by the grant AIRC IG16930. AS, OE, RZ and RM were supported by a private melanoma research donation from Liechtenstein and RM was further supported by two network grants SFB-F061 and SFB-F047 and RS, KK, MV and MM were supported by P 25336-B13, all from the Austrian Science Fund (FWF).

References

1. Siegel RL, Miller KD, Jemal A. Cancer statistics, 2016. *CA: a cancer journal for clinicians*. 2016; 66:7–30. [PubMed: 26742998]
2. Hoek KS, Eichhoff OM, Schlegel NC, Dobbeling U, Kobert N, Schaerer L, et al. In vivo switching of human melanoma cells between proliferative and invasive states. *Cancer research*. 2008; 68:650–656. [PubMed: 18245463]
3. Kemper K, de Goeje PL, Peeper DS, van Amerongen R. Phenotype switching: tumor cell plasticity as a resistance mechanism and target for therapy. *Cancer research*. 2014; 74:5937–5941. [PubMed: 25320006]

4. Li FZ, Dhillon AS, Anderson RL, McArthur G, Ferrao PT. Phenotype switching in melanoma: implications for progression and therapy. *Frontiers in oncology*. 2015; 5:31. [PubMed: 25763355]
5. Yasumoto K, Yokoyama K, Shibata K, Tomita Y, Shibahara S. Microphthalmia-associated transcription factor as a regulator for melanocyte-specific transcription of the human tyrosinase gene. *Mol Cell Biol*. 1994; 14:8058–8070. [PubMed: 7969144]
6. Hemesath TJ, Steingrimsson E, McGill G, Hansen MJ, Vaught J, Hodgkinson CA, et al. microphthalmia, a critical factor in melanocyte development, defines a discrete transcription factor family. *Genes Dev*. 1994; 8:2770–2780. [PubMed: 7958932]
7. Steingrimsson E, Copeland NG, Jenkins NA. Melanocytes and the microphthalmia transcription factor network. *Annu Rev Genet*. 2004; 38:365–411. [PubMed: 15568981]
8. Carreira S, Goodall J, Denat L, Rodriguez M, Nuciforo P, Hoek KS, et al. Mitf regulation of Dial controls melanoma proliferation and invasiveness. *Genes Dev*. 2006; 20:3426–3439. [PubMed: 17182868]
9. Goodall J, Carreira S, Denat L, Kobi D, Davidson I, Nuciforo P, et al. Brn-2 represses microphthalmia-associated transcription factor expression and marks a distinct subpopulation of microphthalmia-associated transcription factor-negative melanoma cells. *Cancer research*. 2008; 68:7788–7794. [PubMed: 18829533]
10. Verfaillie A, Imrichova H, Atak ZK, Dewaele M, Rambow F, Hulselmans G, et al. Decoding the regulatory landscape of melanoma reveals TEADS as regulators of the invasive cell state. *Nature communications*. 2015; 6:6683.
11. Kortylewski M, Jove R, Yu H. Targeting STAT3 affects melanoma on multiple fronts. *Cancer Metastasis Rev*. 2005; 24:315–327. [PubMed: 15986140]
12. Fofaria NM, Srivastava SK. Critical role of STAT3 in melanoma metastasis through anoikis resistance. *Oncotarget*. 2014; 5:7051–7064. [PubMed: 25216522]
13. Niu G, Heller R, Catlett-Falcone R, Coppola D, Jaroszeski M, Dalton W, et al. Gene therapy with dominant-negative Stat3 suppresses growth of the murine melanoma B16 tumor in vivo. *Cancer research*. 1999; 59:5059–5063. [PubMed: 10537273]
14. Kortylewski M, Heinrich PC, Mackiewicz A, Schniertshauer U, Klingmuller U, Nakajima K, et al. Interleukin-6 and oncostatin M-induced growth inhibition of human A375 melanoma cells is STAT-dependent and involves upregulation of the cyclin-dependent kinase inhibitor p27/Kip1. *Oncogene*. 1999; 18:3742–3753. [PubMed: 10391682]
15. Lacreusette A, Nguyen JM, Pandolfino MC, Khammari A, Dreno B, Jacques Y, et al. Loss of oncostatin M receptor beta in metastatic melanoma cells. *Oncogene*. 2007; 26:881–892. [PubMed: 16909117]
16. Grabner B, Schramek D, Mueller KM, Moll HP, Svinka J, Hoffmann T, et al. Disruption of STAT3 signalling promotes KRAS-induced lung tumorigenesis. *Nature communications*. 2015; 6:6285.
17. Musteanu M, Blaas L, Mair M, Schleder M, Bilban M, Tauber S, et al. Stat3 is a negative regulator of intestinal tumor progression in Apc(Min) mice. *Gastroenterology*. 2010; 138:1003–1011. [PubMed: 19962983]
18. Pencik J, Schleder M, Gruber W, Unger C, Walker SM, Chalaris A, et al. STAT3 regulated ARF expression suppresses prostate cancer metastasis. *Nature communications*. 2015; 6:7736.
19. Ackermann J, Fruttschi M, Kaloulis K, McKee T, Trumpp A, Beermann F. Metastasizing melanoma formation caused by expression of activated N-RasQ61K on an INK4a-deficient background. *Cancer research*. 2005; 65:4005–4011. [PubMed: 15899789]
20. Genomic Classification of Cutaneous Melanoma. *Cell*. 2015; 161:1681–1696. [PubMed: 26091043]
21. Alonzi T, Maritano D, Gorgoni B, Rizzuto G, Libert C, Poli V. Essential role of STAT3 in the control of the acute-phase response as revealed by inducible gene inactivation [correction of activation] in the liver. *Mol Cell Biol*. 2001; 21:1621–1632. [PubMed: 11238899]
22. Serrano M, Lee H, Chin L, Cordon-Cardo C, Beach D, DePinho RA. Role of the INK4a locus in tumor suppression and cell mortality. *Cell*. 1996; 85:27–37. [PubMed: 8620534]
23. Delmas V, Martinozzi S, Bourgeois Y, Holzenberger M, Larue L. Cre-mediated recombination in the skin melanocyte lineage. *Genesis*. 2003; 36:73–80. [PubMed: 12820167]

24. Luciani F, Champeval D, Herbette A, Denat L, Aylaj B, Martinozzi S, et al. Biological and mathematical modeling of melanocyte development. *Development*. 2011; 138:3943–3954. [PubMed: 21862558]
25. Jeffs AR, Glover AC, Slobbe LJ, Wang L, He S, Hazlett JA, et al. A gene expression signature of invasive potential in metastatic melanoma cells. *PLoS One*. 2009; 4:e8461. [PubMed: 20041153]
26. Strub T, Giuliano S, Ye T, Bonet C, Keime C, Kobi D, et al. Essential role of microphthalmia transcription factor for DNA replication, mitosis and genomic stability in melanoma. *Oncogene*. 2011; 30:2319–2332. [PubMed: 21258399]
27. Subramanian A, Tamayo P, Mootha VK, Mukherjee S, Ebert BL, Gillette MA, et al. Gene set enrichment analysis: a knowledge-based approach for interpreting genome-wide expression profiles. *Proc Natl Acad Sci U S A*. 2005; 102:15545–15550. [PubMed: 16199517]
28. Matsuda T, Nakamura T, Nakao K, Arai T, Katsuki M, Heike T, et al. STAT3 activation is sufficient to maintain an undifferentiated state of mouse embryonic stem cells. *EMBO J*. 1999; 18:4261–4269. [PubMed: 10428964]
29. Aguirre-Gamboa R, Gomez-Rueda H, Martinez-Ledesma E, Martinez-Torteya A, Chacolla-Huaringa R, Rodriguez-Barrientos A, et al. SurvExpress: an online biomarker validation tool and database for cancer gene expression data using survival analysis. *PLoS One*. 2013; 8:e74250. [PubMed: 24066126]
30. Lambert AW, Pattabiraman DR, Weinberg RA. Emerging Biological Principles of Metastasis. *Cell*. 2017; 168:670–691. [PubMed: 28187288]
31. Igelmann S, Neubauer HA, Ferbeyre G. STAT3 and STAT5 Activation in Solid Cancers. *Cancers (Basel)*. 2019:11.
32. Ladstein RG, Bachmann IM, Straume O, Akslen LA. Ki-67 expression is superior to mitotic count and novel proliferation markers PHH3, MCM4 and mitotin as a prognostic factor in thick cutaneous melanoma. *BMC cancer*. 2010; 10:140. [PubMed: 20398247]
33. Tu TJ, Ma MW, Monni S, Rose AE, Yee H, Darvishian F, et al. A high proliferative index of recurrent melanoma is associated with worse survival. *Oncology*. 2011; 80:181–187. [PubMed: 21701232]
34. Garraway LA, Widlund HR, Rubin MA, Getz G, Berger AJ, Ramaswamy S, et al. Integrative genomic analyses identify MITF as a lineage survival oncogene amplified in malignant melanoma. *Nature*. 2005; 436:117–122. [PubMed: 16001072]
35. Goding CR, Arnheiter H. MITF—the first 25 years. *Genes Dev*. 2019; 33:983–1007. [PubMed: 31123060]
36. Yamada T, Tobita K, Osada S, Nishihara T, Imagawa M. CCAAT/enhancer-binding protein delta gene expression is mediated by APRF/STAT3. *J Biochem*. 1997; 121:731–738. [PubMed: 9163525]
37. Lee M, Goodall J, Verastegui C, Ballotti R, Goding CR. Direct regulation of the Microphthalmia promoter by Sox10 links Waardenburg-Shah syndrome (WS4)-associated hypopigmentation and deafness to WS2. *J Biol Chem*. 2000; 275:37978–37983. [PubMed: 10973953]
38. Verastegui C, Bille K, Ortonne JP, Ballotti R. Regulation of the microphthalmia-associated transcription factor gene by the Waardenburg syndrome type 4 gene, SOX10. *J Biol Chem*. 2000; 275:30757–30760. [PubMed: 10938265]
39. Qi X, Hong J, Chaves L, Zhuang Y, Chen Y, Wang D, et al. Antagonistic regulation by the transcription factors C/EBPalpha and MITF specifies basophil and mast cell fates. *Immunity*. 2013; 39:97–110. [PubMed: 23871207]
40. Shenoy AK, Jin Y, Luo H, Tang M, Pampo C, Shao R, et al. Epithelial-to-mesenchymal transition confers pericyte properties on cancer cells. *J Clin Invest*. 2016; 126:4174–4186. [PubMed: 27721239]
41. Ohanna M, Cheli Y, Bonet C, Bonazzi VF, Allegra M, Giuliano S, et al. Secretome from senescent melanoma engages the STAT3 pathway to favor reprogramming of naive melanoma towards a tumor-initiating cell phenotype. *Oncotarget*. 2013; 4:2212–2224. [PubMed: 24344100]
42. Steder M, Alla V, Meier C, Spitschak A, Pahnke J, Furst K, et al. DNp73 exerts function in metastasis initiation by disconnecting the inhibitory role of EPLIN on IGF1R-AKT/STAT3 signaling. *Cancer cell*. 2013; 24:512–527. [PubMed: 24135282]

43. Lee JW, Stone ML, Porrett PM, Thomas SK, Komar CA, Li JH, et al. Hepatocytes direct the formation of a pro-metastatic niche in the liver. *Nature*. 2019; 567:249–252. [PubMed: 30842658]
44. Cao HH, Chu JH, Kwan HY, Su T, Yu H, Cheng CY, et al. Inhibition of the STAT3 signaling pathway contributes to apigenin-mediated anti-metastatic effect in melanoma. *Scientific reports*. 2016; 6:21731. [PubMed: 26911838]
45. Weidenfeld K, Barkan D. EMT and Stemness in Tumor Dormancy and Outgrowth: Are They Intertwined Processes? *Frontiers in oncology*. 2018; 8:381. [PubMed: 30258818]
46. Tang Y, Luo Y, Jiang Z, Ma Y, Lin CJ, Kim C, et al. Jak/Stat3 signaling promotes somatic cell reprogramming by epigenetic regulation. *Stem Cells*. 2012; 30:2645–2656. [PubMed: 22968989]
47. Huser L, Sachindra S, Granados K, Federico A, Larribere L, Novak D, et al. SOX2-mediated upregulation of CD24 promotes adaptive resistance toward targeted therapy in melanoma. *International journal of cancer*. 2018; 143:3131–3142. [PubMed: 29905375]
48. Gong AH, Wei P, Zhang S, Yao J, Yuan Y, Zhou AD, et al. FoxM1 Drives a Feed-Forward STAT3-Activation Signaling Loop That Promotes the Self-Renewal and Tumorigenicity of Glioblastoma Stem-like Cells. *Cancer research*. 2015; 75:2337–2348. [PubMed: 25832656]
49. He W, Wu J, Shi J, Huo YM, Dai W, Geng J, et al. IL22RA1/STAT3 Signaling Promotes Stemness and Tumorigenicity in Pancreatic Cancer. *Cancer research*. 2018; 78:3293–3305. [PubMed: 29572224]
50. Tang Y, Kitisin K, Jogunoori W, Li C, Deng CX, Mueller SC, et al. Progenitor/stem cells give rise to liver cancer due to aberrant TGF-beta and IL-6 signaling. *Proc Natl Acad Sci U S A*. 2008; 105:2445–2450. [PubMed: 18263735]
51. Kulesza DW, Przanowski P, Kaminska B. Knockdown of STAT3 targets a subpopulation of invasive melanoma stem-like cells. *Cell Biol Int*. 2019; 43:613–622. [PubMed: 30958597]
52. Anastas JN, Kulikauskas RM, Tamir T, Rizos H, Long GV, von Euw EM, et al. WNT5A enhances resistance of melanoma cells to targeted BRAF inhibitors. *J Clin Invest*. 2014; 124:2877–2890. [PubMed: 24865425]
53. Kudo-Saito C, Shirako H, Takeuchi T, Kawakami Y. Cancer metastasis is accelerated through immunosuppression during Snail-induced EMT of cancer cells. *Cancer cell*. 2009; 15:195–206. [PubMed: 19249678]
54. Bu X, Mahoney KM, Freeman GJ. Learning from PD-1 Resistance: New Combination Strategies. *Trends in molecular medicine*. 2016; 22:448–451. [PubMed: 27174038]
55. Ji Z, Erin Chen Y, Kumar R, Taylor M, Jenny Njauw CN, Miao B, et al. MITF Modulates Therapeutic Resistance through EGFR Signaling. *J Invest Dermatol*. 2015; 135:1863–1872. [PubMed: 25789707]
56. Mirea MA, Eckensperger S, Hengstschlager M, Mikula M. Insights into Differentiation of Melanocytes from Human Stem Cells and Their Relevance for Melanoma Treatment. *Cancers (Basel)*. 2020:12.
57. Kinslechner K, Schutz B, Pistek M, Rapolter P, Weitzenbock HP, Hundsberger H, et al. Loss of SR-BI Down-Regulates MITF and Suppresses Extracellular Vesicle Release in Human Melanoma. *International journal of molecular sciences*. 2019:20.
58. Yokoyama S, Feige E, Poling LL, Levy C, Widlund HR, Khaled M, et al. Pharmacologic suppression of MITF expression via HDAC inhibitors in the melanocyte lineage. *Pigment cell & melanoma research*. 2008; 21:457–463. [PubMed: 18627530]

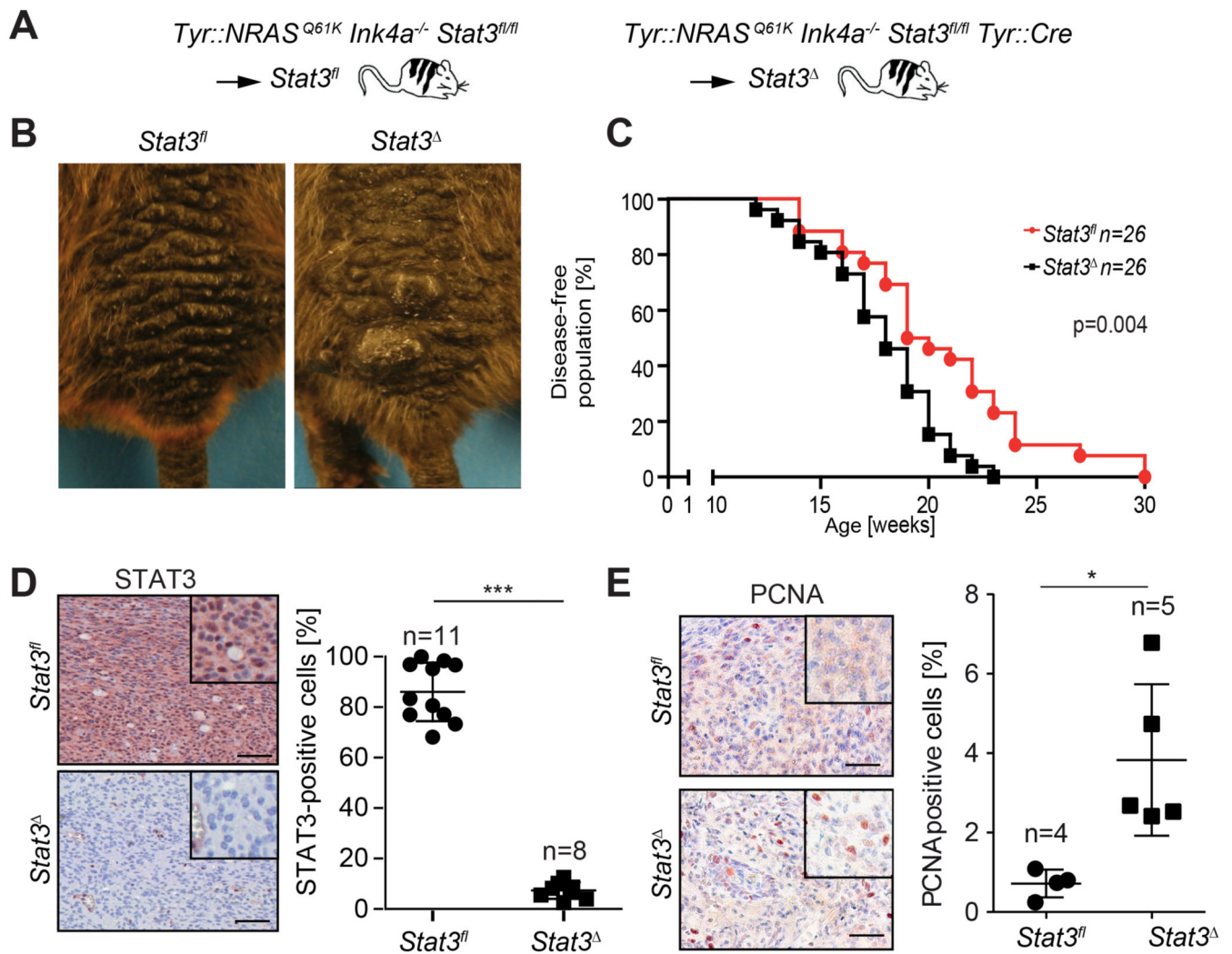


Fig. 1. STAT3 knockout in melanoma induced earlier tumor onset, but reduced metastasis.

a Mice containing a constitutively active *NRAS* gene controlled by the *tyrosinase* promoter and a deletion of the *Ink4a* locus were crossed to mice harboring a *floxed Stat3* locus termed “Stat3^{fl/fl}”. Mice additionally expressing *Cre* recombinase by a *tyrosinase* promoter were termed “Stat3^Δ”. **b** Representative pictures of 20 week-old mice. **c** Logrank (Mantel-Cox) test was used to display Kaplan–Meier plot, showing disease-free survival, defined as time before palpable tumors occur, of Stat3^{fl/fl} mice compared to the Stat3^Δ group. **d+e** IHC evaluation of total STAT3 and PCNA in primary melanoma of Stat3^{fl/fl} and Stat3^Δ mice. Scale bars, 50 μm. Data are shown as mean ± sd. *P* values represent Mann-Whitney U test. ***, *P* < 0.001, *, *P* < 0.05.

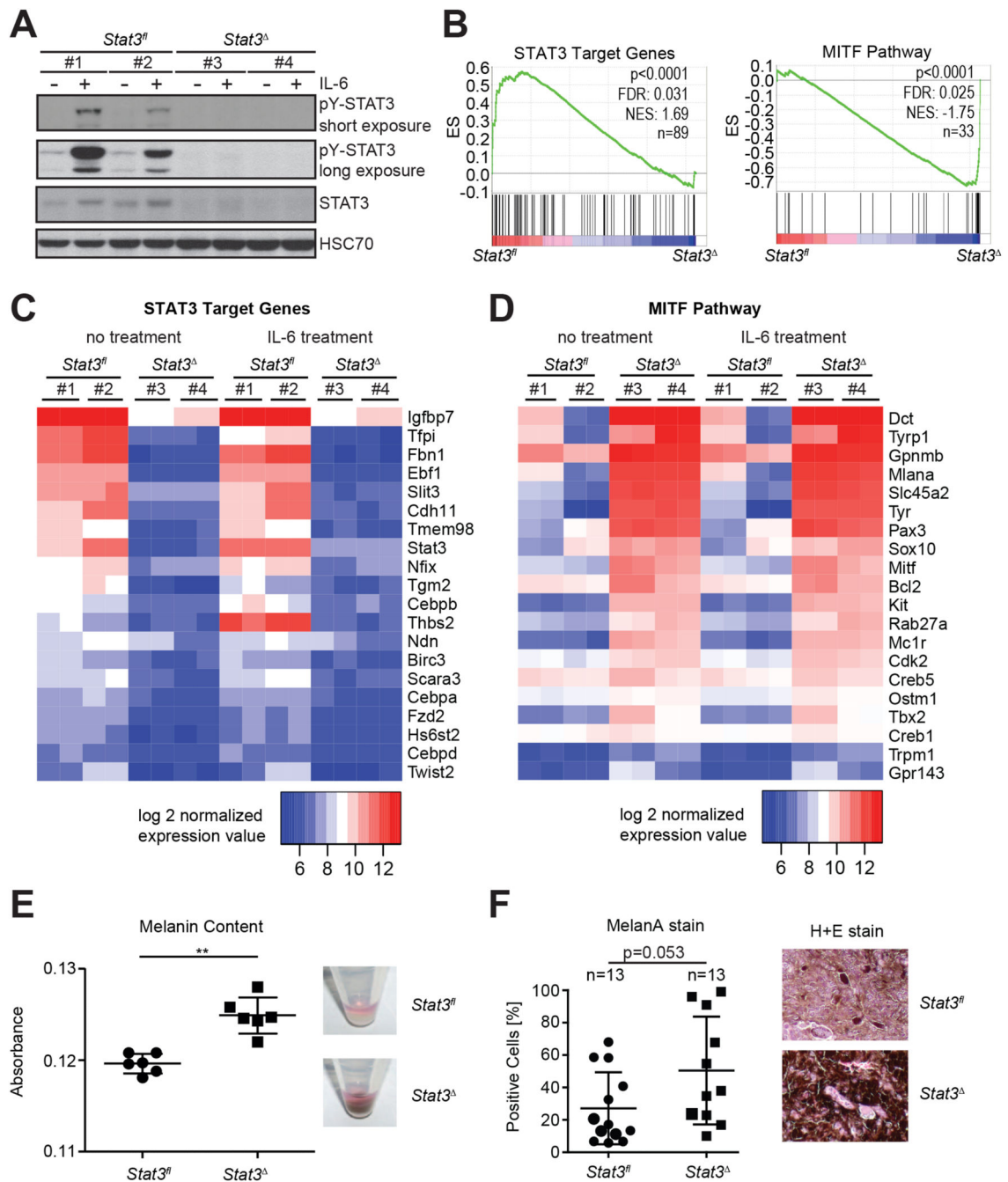


Fig. 2. Loss of *Stat3* induced MITF pathway in melanoma cells.

a Representative Western blot showing total STAT3 levels and IL-6 stimulated (20 ng/ml, 30 minutes) STAT3 phosphorylation at Y705 in two representative cell lines derived from either *Stat3^{fl}* (#1 and #2) or *Stat3^Δ* tumors (#3 and #4). HSC70 served as loading control. **b** 89 STAT3 target genes and 33 genes in the MITF pathway were evaluated by gene-set enrichment analysis (GSEA) during normal growth in cell culture. **c** Heatmap showing the top 20 regulated genes of the STAT3 gene-set. **d** Heatmap of the top 20 regulated genes of the MITF gene-set. **e** Melanin content in supernatant from tumor derived mouse melanoma

cell lines, after 48 hours of culturing, was measured by absorption at 410 nm. Results represent six independent measurements. **f** Tissue sections of primary tumors were stained by anti-MelanA antibody and percentage of positive cells is shown (left). Representative section, indicating melanin content, is shown (right). In e and f data are shown as mean \pm sd. *P* values represent Mann-Whitney U test. **, *P* < 0.01.

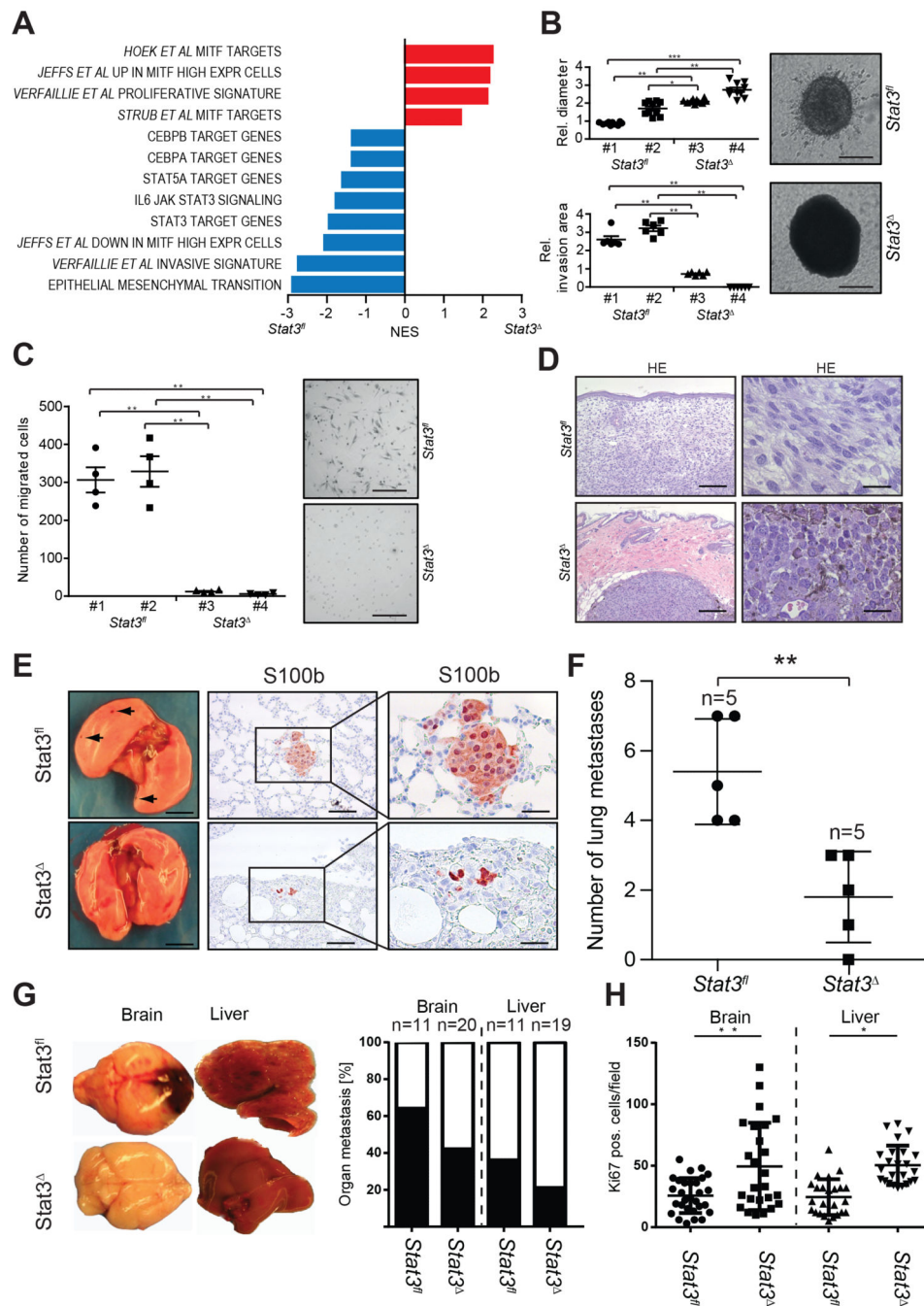


Fig. 3. Transcriptome analysis and functional testing revealed abrogated invasion and increased proliferation after STAT3 knockout.

a Normalized enrichment scores (NES) calculated for gene signatures derived from the GSEA database (H and C3) or from publications (first author is listed) with a false discovery rate <5% and $p < 0.05$. **b** 3D-proliferation and sphere invasion assay of Stat3^{fl/fl} and Stat3^{-/-} melanoma cells into a collagen gel (n=10/group). Stat3^{-/-} cells proliferate faster (upper panel) and have abrogated invasive capabilities (n=6/group) (lower panel). Two representative spheres are displayed. Scale bar, 200 μ m. **c** Transwell migration assay of Stat3^{fl/fl} and Stat3^{-/-}

melanoma cells (n=4). STAT3 deletion leads to abrogated migration. Scale bar, 100 μm . **d** Representative HE stainings of tumors formed from Stat3^{fl} and Stat3^{-/-} cells grafted into NSG mice. Subcutaneously injected tumors of the Stat3^{fl} group invaded the dermis, while tumors of the Stat3^{-/-} group have a compact structure with even borders that did not invade into the dermis. Scale bar (left), 300 μm , scale bar (right), 20 μm . **e** Representative lungs, arrows indicate melanoma metastases (left); S100b staining (right). Scale bar (left), 3 mm, scale bar (middle), 150 μm , scale bar (right), 60 μm . **f** Metastasis quantification of age matched lung samples of Stat3^{fl} and Stat3^{-/-} mice, showing a total of **27 lung metastatic lesions in WT and 9 in KO mice**. **g** Representative pictures for brain and liver metastasis (left). Distribution of organ metastasis in Stat3^{fl} and Stat3^{-/-} genotypes (right). **h** Total number of KI67 positive tumor cells per field of 500 tumor cells. 6 individual tumor samples per genotype were analyzed in four random areas. In b, c, f and h data are shown as mean \pm sd. *P* values represent Mann-Whitney U test. ***, *P* < 0.001, **, *P* < 0.01, *, *P* < 0.05.

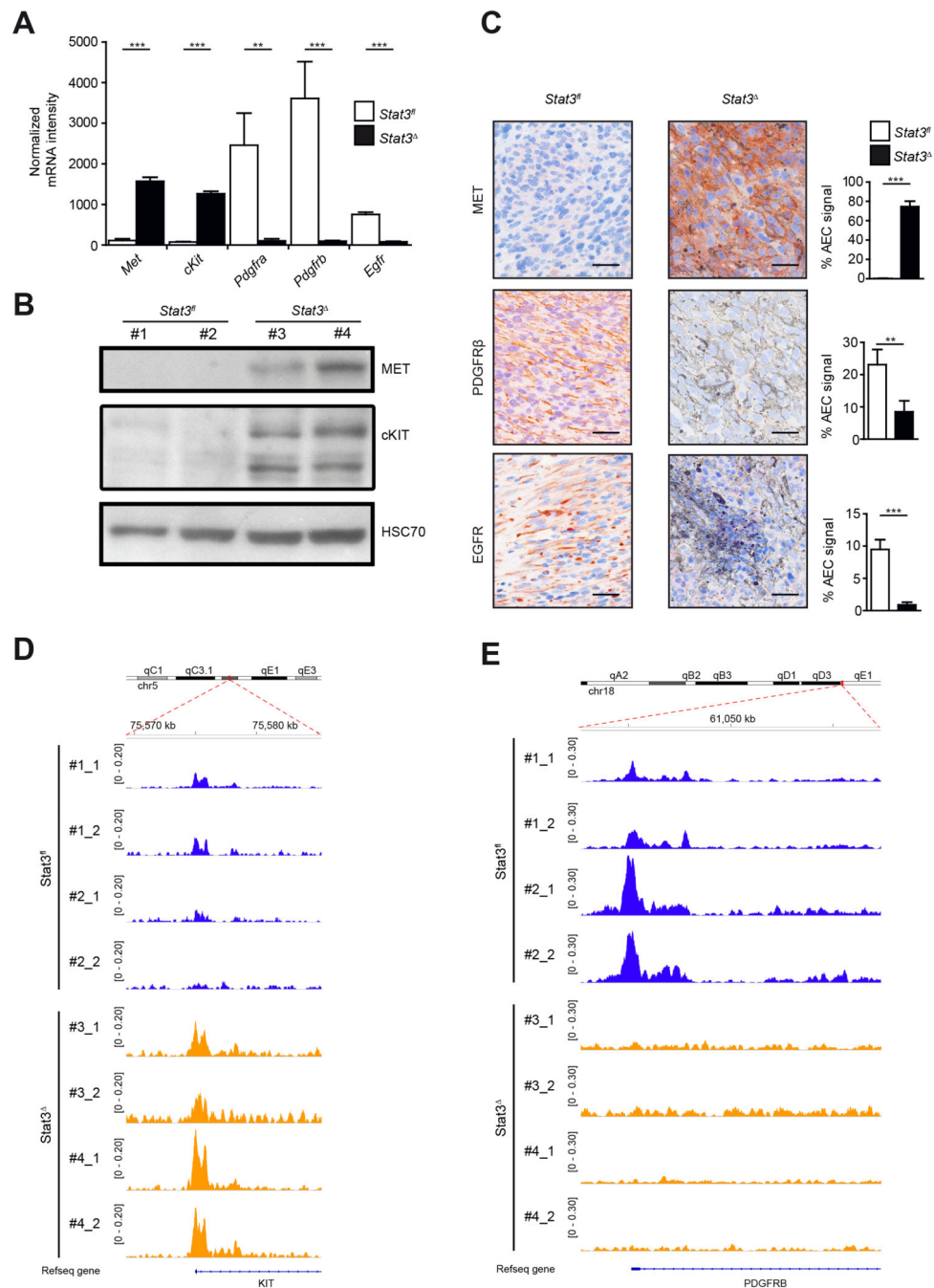


Fig. 4. Expression of receptor tyrosine kinases display a YIN/YANG dualism corresponding to STAT3/MITF interplay.

a The total mRNA levels of a set of significantly regulated RTK related to STAT3 and MITF signaling after normalization of the whole transcriptome expression screen comparing the expression levels between the Stat3^{fl} and the Stat3^{-/-} group. Bar charts show mean expression intensity \pm sd of 6 samples per group. **b** Western blot of two Stat3 wild type (#1 and #2) and two knock out cell lines (#3 and #4) for MET and cKIT. HSC70 served as loading control. **c** Representative images of antibody stainings in tumors derived of grafted Stat3^{fl} and Stat3^{-/-}

cell lines in NSG mice. Red color depicts specific immunostaining and black/brown is related to pigmentation. Scale bar, 25 μ m. Bar charts showing AEC signal mean \pm sd of 4 samples per group. **d+e** ATAC-seq signal intensities at the *cKit* and at the *Pdgfra* locus. Two independent cell lines with biological duplicates are depicted in blue as STAT3^{fl} and in yellow as STAT3^{+/+}. *P* values represent Mann-Whitney U test. ***, *P* < 0.001, **, *P* < 0.01, *, *P* < 0.05.

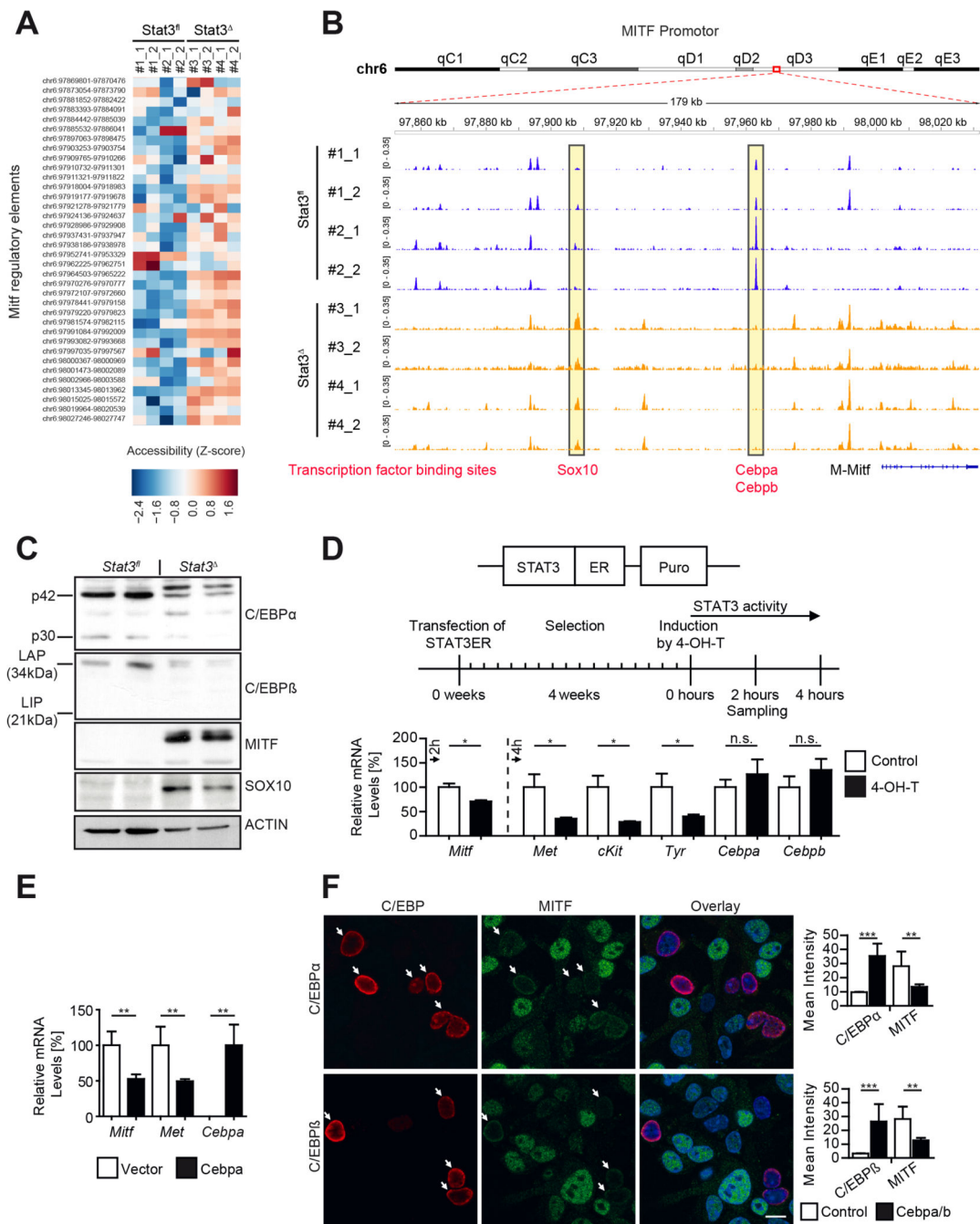


Fig. 5. MITF expression depends on the STAT3 target *Cebpa* and *Cebpb*.

a Heatmap displays the grade of accessible chromatin from MITF regulatory elements. Blue correlates with closed or less accessible chromatin and red with open or more accessible chromatin for binding factors. **b** ATAC-seq signal intensities at the M-MITF locus and the possible binding sites of SOX10 and CEBPa/b. Data mapped according to ChIP-Atlas. Depicted in blue are Stat3^{fl} cell lines and in yellow Stat3⁻ cell lines all in technical duplicates. **c** Western blots show increased expression of both the 42 kDa (p42) and the 30 kDa (p30) isoform of CEBPa/b and decreased expression of MITF and SOX10 in Stat3^{fl}

cells in comparison to the Stat3^{fl} group. Actin served as loading control. **d** Lipofectamine transfection and stable selection via puromycin of Stat3^{fl} murine melanoma cells with a STAT3ER^{T2} construct that can be activated by 4-Hydroxytamoxifen (4-OH-T). MITF pathway is down-regulated after two to four hours after activation with 1 μ M 4-OH-T. Bar charts shows mean expression intensity \pm sd of 4 samples per group **e** *Mitf* and *Met* regulation after 24 hours transient *Cebpa* transfection of murine Stat3^{fl} cells by lipofectamine. Bar charts shows mean expression intensity \pm sd of 4 samples per group. **f** Co-immunofluorescence for CEBPa or CEBPb and MITF expression after transient *Cebpa* or *Cebpb* transfection by lipofectamine for 24 hours in Stat3^{fl} murine melanoma cells. Scale bar, 5 μ m. Quantification of cells expressing CEBPa or CEBPb by showing mean intensity \pm sd of 10 samples per group. *P* values represent Mann-Whitney U test. ***, *P* < 0.001, **, *P* < 0.01, *, *P* < 0.05, ns, not significant.

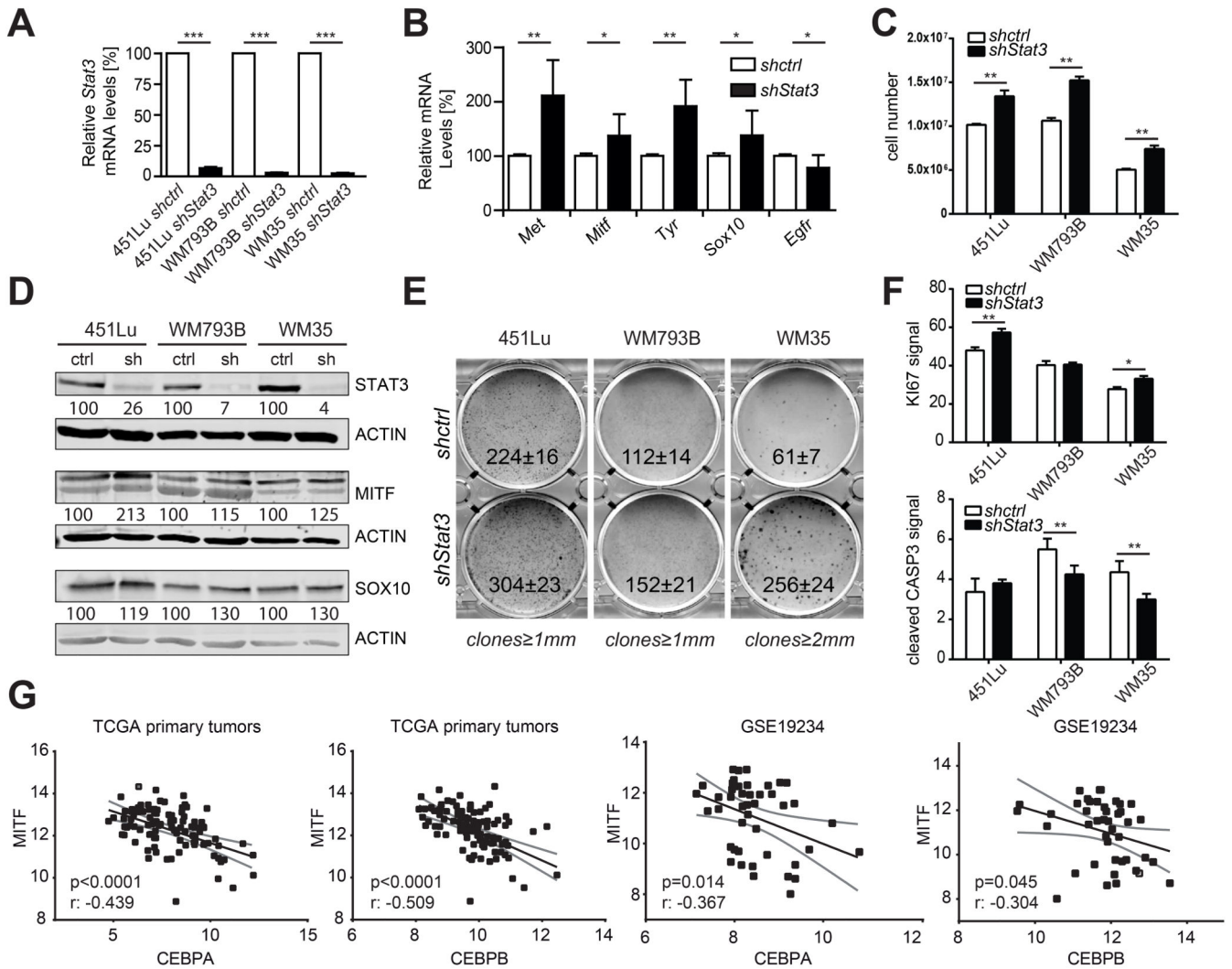


Fig. 6. Human melanoma cells induce MITF and proliferation upon loss of STAT3.

Three human melanoma cell lines were transduced with *STAT3* shRNA or a scrambled control by lentivirus and selected via puromycin resistance. **a** Evaluation *STAT3* RNA amounts by RT-PCR. **b** mRNA expression of MITF pathway members was up-regulated upon *STAT3* silencing in WM35 cells. **c** Of each cell line 10⁶ cells were seeded and after 4 days of culturing cell number was measured. **d** Evaluation of the *shSTAT3* RNA knockdown by Western blot for *STAT3*, *SOX10* and *MITF* levels. Actin served as loading control. Numbers depict normalized intensity levels. **e** Of each cell line 10⁴ cells were used for a clonogenic growth assay. After 10 days of growth colonies were fixed and stained with crystal violet. Three independent samples were counted, mean ± sd is shown. **f** Each line was seeded in 96 well plates and stained with anti-Ki67 and anti-cleaved caspase 3 antibodies. Normalized fluorescence signals are shown. **g** Data from the publicly available “the cancer genome atlas – skin cutaneous melanoma (TCGA-SKCM)” and “GSE19234” human malignant melanoma patient datasets (Bogunovic, TCGA) were tested for correlations between *CEBPA* vs. *MITF* and *CEBPB* vs. *MITF* by calculating Pearson correlation coefficients. Data in a, b, c and f are bar charts showing mean expression

intensity \pm sd of 4 samples per group. *P* values represent Mann-Whitney U test. ***, *P* < 0.001, **, *P* < 0.01, *, *P* < 0.05.

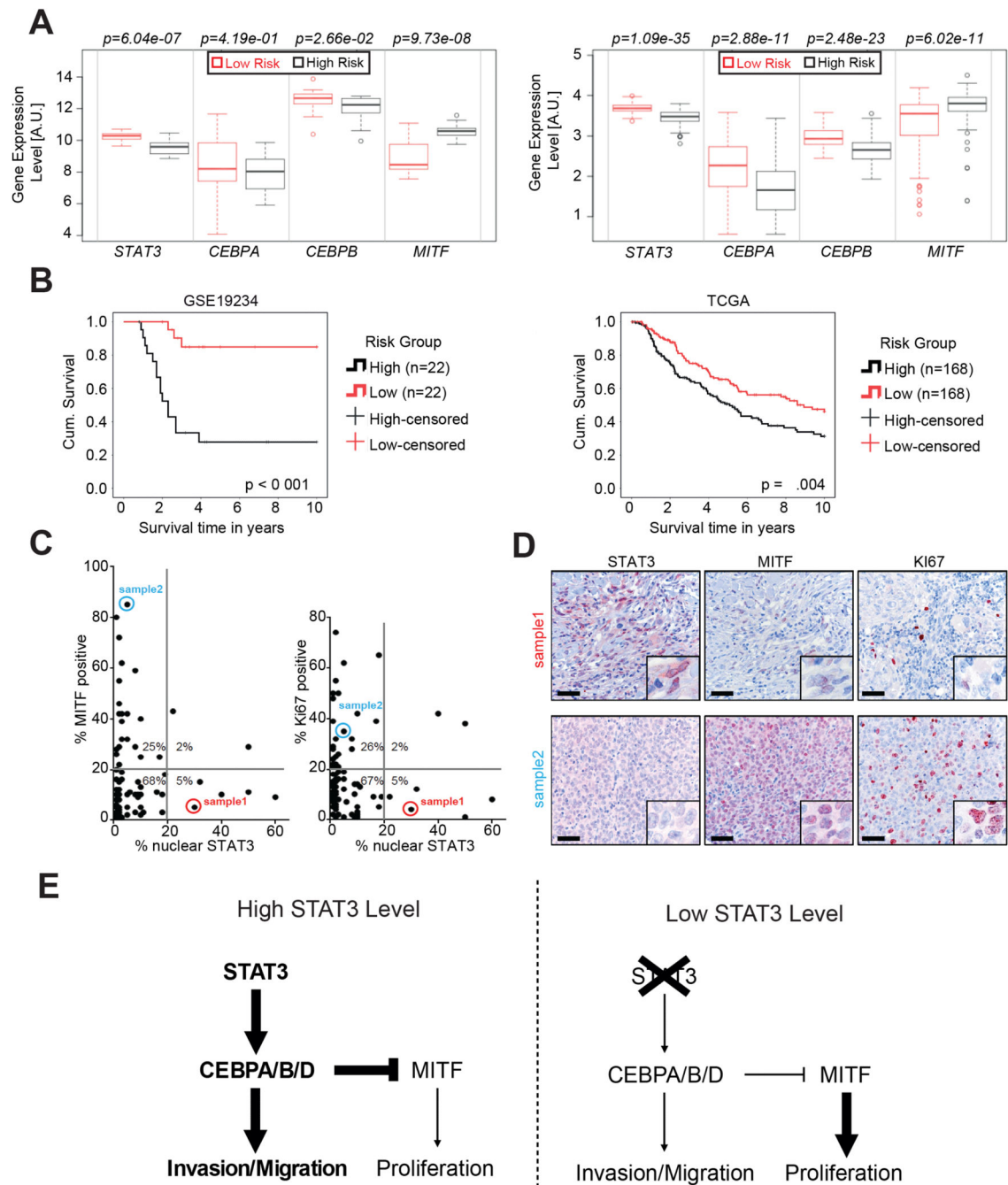


Fig. 7. Human patients with $STAT3^{\text{low}}$, $CEBPA^{\text{low}}$, $CEBPB^{\text{low}}$ and $MITF^{\text{high}}$ signature show worsened clinical outcome.

a Box-Whisker plot of mean gene expression levels of *STAT3*, *CEBPA*, *CEBPB* and *MITF*, which were determined by survexpress to result in a maximum survival probability difference between low- and high-risk groups. Datasets were used from *Bogunovic* et al. (44 samples, GSE19234) and the TCGA-SKCM (336 samples). **b** Kaplan-Meier analysis of high- and low-risk groups as defined in a. **c** A group of 98 melanoma metastasis samples were stained for STAT3, MITF and KI67. Each sample was evaluated for the distribution of

nuclear STAT3, as well as MITF and KI67. **d** Two representative tissue samples (sample1 for high nuclear STAT3 and sample2 for low nuclear STAT3) are shown with three consecutive sections, which were stained for STAT3, MITF and KI67. Scale bars, 50 μm . **e** Scheme depicting changes in transcription factor interaction governing the melanoma phenotype. In Stat3^{fl} mice, STAT3 pathway is active, EGFR and PDGFRa/b is up-regulated and an EMT-like melanoma phenotype persists. When STAT3 activity is low or absent, MITF is released from suppression by CEBP family members. Subsequently, MITF target genes like *cKIT* and *MET* are up-regulated and proliferation of melanoma is enhanced.